EXTERNAL ROTOR RELUCTANCE MACHINE FOR A KINETIC ENERGY STORAGE SYSTEM

EDUARDO BERNSMÜLLER

Brazilian Navy Research Institute (IPqM), Weapons Systems/Electronics and Computing Division.
Ilha do Governador, 21931090 – Rio de Janeiro, RJ – Brazil.
E-mail: eduberns@yahoo.com.br

LUÍS G. B. ROLIM, ANTÔNIO C. FERREIRA

Department of Electrical Engineering – COPPE , Universidade Federal do Rio de Janeiro (UFRJ).
Cidade Universitária, 21941972 – Rio de Janeiro, RJ – Brazil.
E-mails: rolim@ufrj.br, ferreira@ufrj.br

Abstract— This paper presents the design steps of a switched reluctance machine, as the specification of its basic requirements, the electromagnetic design, the modeling and the validation through magnetostatic and dynamic finite element simulations method. The switched reluctance machine has an external rotor that should operate up to 50,000 revolutions per minute and is applied as a flywheel in a Kinetic Energy Storage System. A rated load of one kilowatt is supplied by the flywheel through a 300 volt direct current link.

Keywords— Power electronics, Reluctance machine, External rotor, Outer rotor, Kinetic energy storage system.

1 Introduction

Among the many possible commercial applications of switched reluctance machines (SRMs) is the Kinetic Energy Storage System, also called Flywheel Energy Storage System (FESS). Figure 1 shows an overview of the proposed FESS for analysis and design in this work.

The Main Power Supply provides power to a constant, 300 volt DC Link through a rectifier. This same link also feeds the critical load and excites the reluctance machine through its converter. In this condition, the machine operates as a motor rotating at rated speed.

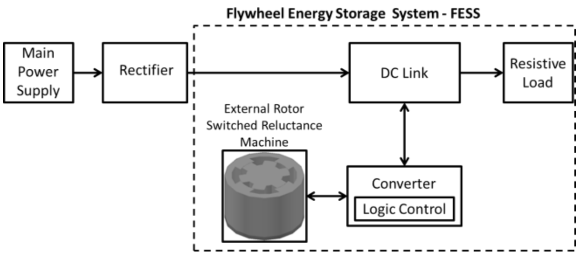

Figure 1: Overview of proposed FESS.

When an outage of the main power occurs, the SRM operates as a generator, converting the kinetic energy of its rotor into electric energy, supplying power to the critical load. This operation mode lasts the time needed to a gas or diesel back-up generator to start.

This paper presents the requirement specifications, summarizes the design procedure of a switched reluctance machine, describes the modeling of drivers and the results of Finite Element Method (FEM) simulations coupled to dynamic simulations of the converter and controllers. Different from commercial products (Active Power; POWERTHRU; Vyco Energy) the designed SRM has an external rotor and is applied to a high speed FESS. Since the rotor has a larger radius comparing to an equivalent internal rotor machine, it has greater moment of inertia. The rotor can play the function of flywheel, simplifying the mechanical project. This paper presents the initial development and simulations of a machine designed to incorporate in the future the concept of self-bearing, producing electromagnetic torque and restoration forces by the same coils (Ortiz, 1989).

2 Requirements specification

In this section the FESS requirements are defined, based on commercial products (Active Power; POWERTHRU; Vyco Energy).

The first requirement assumes a time of 120 s for FESS to accelerate from rest to full speed. Considering also a typical time of 10 s (Zanei, 2007) for a diesel back-up generator to start, it was defined that the FESS should power a critical load for a minimum of 15 s.

The overall objective is to develop a compact, scalable system. Thus, the external rotor should play the flywheel function. To store sufficient kinetic energy to power the load within the specified time, it must rotate at high speed. Referring to the commercial FESSs, there are models that operate at speeds higher than 50k r/min (POWERTHU). Thus, this speed was set as a design requirement.

To be simple and compact, without external cooling, the current density provided by FESS during flywheel operation mode must be low. For this kind of machine, (Miller, 1993) recommends a 4 A/mm² maximum current density. The output power P_{Ld} is 1 kW supplied from the 300 volt DC Link. The continuous current through the load is 3.33 A. Simulations showed that this current value can be used in the conductor diameter dimensioning.

3 Electromagnetic project

In this section the electromagnetic design procedure of the external rotor SRM is presented in order to meet the specified requirements. Figure 2 shows the definitions of important dimensional variables.

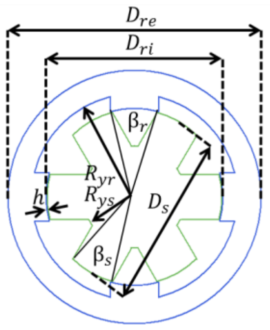

Figure 2: Dimensional variables of the SRM.

Referring to Figure 2: D_{re} and D_{ri} are the internal and external rotor diameter, respectively, D_s is the stator diameter, R_{yr} and R_{ys} are the radii of rotor and stator yoke, respectively, β_r and β_s are the rotor and stator pole arcs, respectively and h is the length of the air gap.

In (Schweitzer, 2002), the author states that it is prudent to maintain tangential speed v_t of the rotor between 250 and 300 m/s to avoid excessive material stress. For v_t ranging between 250 and 300 m/s, and given the angular speed ω_m of 5236 rad/s (50k r/min), the maximum rotor radius r is in the range between 48 and 57 mm. Assuming that initially r is 50 mm long, results in a D_{re} of 100 mm.

The SRM must have at least two phases to allow the radial rotor positioning (Ortiz, 1989). For two phases SRM, the simplest combination is the 4/2 one. The main disadvantage of the two rotor poles machines is the high torque ripple. So these machines should be avoided for a self-bearing application.

The best combination, which in principle meets the project requirements is the three-phase 6/4 one. This configuration has neither null torque regions nor a switching frequency as high as the 8/4 one. This same combination was used in the high-speed dual function motor/generator applied to aircraft, as described in (MacMinn, 1989; Ferreira, 1995; Shoujun, 2010).

For inner rotor motors (Krishnan, 2001), using the relationship given by (1):

$$L_{ri} = k \cdot D_{ri} \tag{1}$$

Where L_{ri} is the active stack length in meters, D_{ri} is the rotor diameter in meters, which will have the same value of the D_{ri} diameter shown in Figure 2. The k constant usually is in the range of 0.25 to 0.7.

Likewise, for an external rotor machine:

$$L_{re} = k \cdot D_{re} \tag{2}$$

The D_{ri} diameter for the external rotor SRM is calculated by the following procedure: assuming for the inner rotor machine the shape of a massive cylinder to the rotor, of which the volume is $V_{ri} = \pi \cdot L_{ri} \cdot {D_{ri}}^2/4$; and assuming to the external rotor machine a form of a hollow cylinder to the rotor, whose volume is $V_{re} = \pi \cdot L_{re} \cdot ({D_{re}}^2 - {D_{ri}}^2)/4$, substituting (1) and (2) in their volume equations and equating the results ($V_{ri} = V_{re}$), gives to the external rotor machine: $D_{ri} = 0.755 \cdot D_{re} = 0.0755$ m.

According to (Shoujun, 2010), a high speed 6/4 motor/generator works suitably with following pole arcs: $\beta_s = 30°$ and $\beta_r = 32°$.

The rotor yoke radius was calculated as the mean of the external and internal rotor radii:

$$R_{yr} = \frac{1}{4} \cdot (D_{re} + D_{ri}) = 0.04388m \tag{3}$$

Assuming a ratio of 20 between the length of the air gap h and the rotor pole length (Shoujun, 2010):

$$h = \frac{1}{20} \cdot \left(R_{yr} - \frac{D_{ri}}{2} \right) = 3.062 \cdot 10^{-4} m \tag{4}$$

Assuming that $h = 0.3$ mm the stator diameter is: $D_s = D_{ri} - 2 \cdot h = 0.0749$ m

The stator yoke radius was set during 2D modeling, leaving enough available area to the coil:

$$R_{ys} = 0.022m \tag{5}$$

Assuming a value of 0.5 for the parameter k and using (2) gives: $L_{re} = 0.05$ m.

After initial simulations, there was the need to adjust the D_{re} value to 108 mm, so the rotor yoke approximately have the minimum recommended width of a half of rotor pole width. The maximum tangential velocity results in 283 m/s.

After assigning the new value to D_{re} and using a 3D solid modeling program, for M-19 silicon-steel and 0.95 stacking factor, it was possible to determine the rotor volume $V_{rot} = 181.39 \cdot 10^{-6}\ m^3$, rotor mass $m_{rot} = 1.318$ kg and rotor moment of inertia $J = 0.00305\ kg \cdot m^2$. Figure 3 shows the SRM 2D model up to this point of the design.

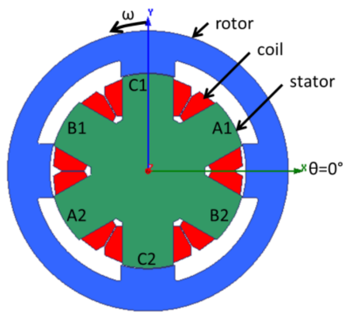

Figure 3: SRM 2D model.

The load current is constant and has the value of 3.33 ampères, as calculated in the previous section. For a 4 A/mm^2 current density (Miller, 1993), the minimum copper area is calculated: $A_{cond} = 3.33/4 = 0.83\ mm^2$. The 17 AWG wire has a 1.04 mm^2 copper area, the 2D model gives 70 mm^2 available area to the coils. So the maximum number of turns per pole N_p, for a 70% maximum fill factor (Krishnan, 2001) is: $N_p = (70/1.04) \cdot 0.7 = 47.1\ turns$. Assuming that the fill factor can be slightly higher, an integer number of 48 turns per pole has been chosen.

4 Magnetostatic simulations

To perform an initial evaluation of the designed SRM, magnetostatic simulations were carried out in ANSYS Maxwell FEM software (ANSYS). This section presents some simulation results. Different constant current values flown through C1 and C2 coils, as shown in Figure 3. The rotor positioning angle, given by *theta* is varied from 0 to 90 mechanical degrees.

4.1 Flux linkages

The flux linkages versus excitation current and rotor positioning characteristics are shown in Figure 4.

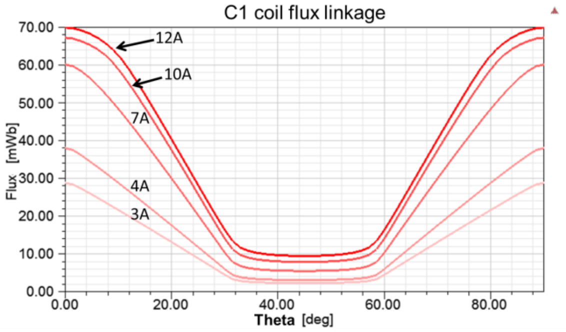

Figure 4: C1 coil flux linkages versus excitation current and rotor *theta* position.

4.2 Self-inductance

Figure 5 shows C1 coil self-inductance versus excitation current and rotor position. It should be noted the saturation effect close to aligned position when a 7, 10 or 12 ampères excitation current flows through the coil. The saliency factor is approximately 7.9.

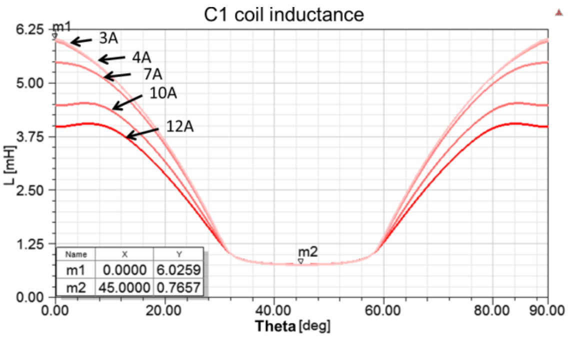

Figure 5: C1 coil self-inductance versus excitation current and rotor *theta* position.

4.3 Torque

Figure 6 shows the rotor's electromagnetic torque versus excitation current and angular position.

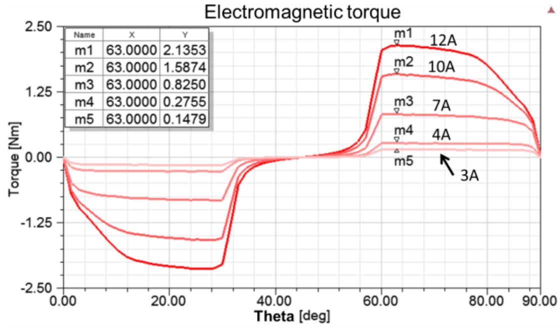

Figure 6: Electromagnetic rotor torque versus excitation current and rotor *theta* position.

The maximum torque for each current value is highlighted. Again the saturation effect causes the torque curves near alignment not to be flat as the excitation currents increases.

5 SRM converter

The SRM asymmetric half bridge converter circuit is shown in Figure 7. It is used in switched reluctance machines, mainly for its simplicity and for allowing the machine to operate as a motor or generator (flywheel). Its operation is well described in (Krishnan, 2001 and Miller, 1993).

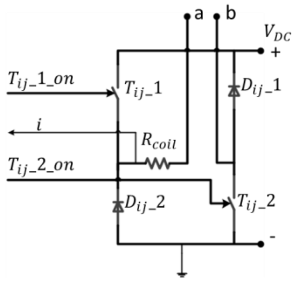

Figure 7: SRM converter circuit.

To allow a future modeling and simulation of the self-bearing technology, it is necessary to excite each stator pole independently (Ortiz, 1989). In this way, the converter is formed by a total of six modules identical to that shown in Figure 7. The other modules are connected in parallel to DC Link.
Terminals "a" and "b" are connected to coil terminals of each pole, whose electromagnetic dynamic model results from Maxwell FEM software. The R_{coil} resistor represents the coil resistance, which was set to a value of 0.14 Ω (@ 75°C), according to the procedure described in (Miller, 1993).

6 Speed controller

While the main power supply is online, the SRM operates as a motor, maintaining the rated speed of 50k r/min. Figure 8 shows the speed controller diagram.

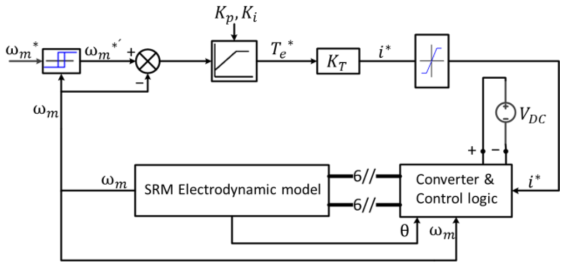

Figure 8: Motor speed controller diagram.

The topology is based on the controller described in (Krishnan, 2001). It consists of a Proportional+Integral controller connected to the SRM converter and its switching logic. The 300 V source represents the DC Link. The $\omega_m{}^*$ speed reference signal is set to 5236 $\mathrm{rad/s}$ and is applied to the input of an 1% hysteresis band comparator. This feature saves power by turning off the converter when the SRM reaches the reference speed and will be depicted later.

The gains were empirically adjusted to $K_p = 0.03$ and $K_i = 1$. The K_T torque constant was determined with the SRM rotating at the nominal speed of 50k r/min, and the i^* reference current was limited to 7 A: $K_T = 0.3\ \mathrm{Nm}/7\ \mathrm{A} = 0.04\ \mathrm{Nm/A}$. The upper limit in coil currents was set to 7 A, which corresponds to a RMS current of $7\ \mathrm{A}/\sqrt{3} \cong 4\ \mathrm{A}$ for a three phase machine, and according to the imposed current density.

Figure 9 shows the electrodynamic model diagram integrated to the SRM FEM model. The electromagnetic torque is given by T_e, J represents the rotor's moment of inertia, Δt is the simulation integration step, B is the viscous friction coefficient arbitrated as $1 \cdot 10^{-6}\ \mathrm{Nm/r \cdot min^{-1}}$ and ω_m is the angular speed. The same model is used in flywheel simulation mode.

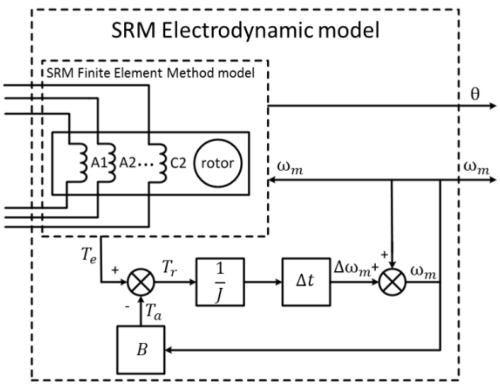

Figure 9: Electrodynamic model diagram.

6.1 *Switched reluctance machine converter control logic in motor mode*

One pole converter control logic integrated to i^* current reference signal, ω_m angular speed and θ rotor position is shown in Figure 10.

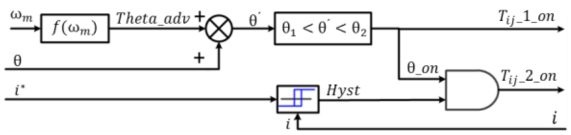

Figure 10: Switched reluctance machine converter control logic in motor mode(one pole).

This logic controls T_{ij}_1 switch to close $Theta\_adv$ mechanical degrees from the beginning of the positive torque region which is defined between θ_1 and θ_2 angles for each pole. The logic also implements a 2% hysteresis band current control, switching T_{ij}_2, applied to instantaneous i current flowing through each coil. The θ_on signal is set as a linear function of ω_m speed and is fixed as 30 mechanical degrees wide. The $Theta\_adv$ angle values between 0 and 10 mechanical degrees, for speeds ranging from 0 to 50k $\mathrm{r/min}$ respectively and compensates the induced back electromotive-force effect on the coil current. Figure 11 shows advance angle and θ_on variation in motor mode.

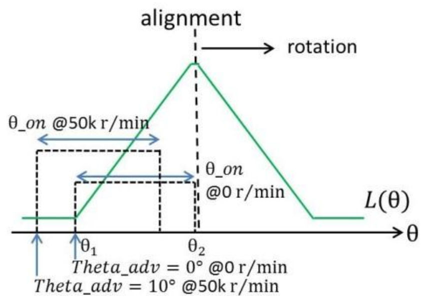

Figure 11: Advance angle and θ_on variation in motor mode.

7 Voltage control

When an outage of the main power occurs, the SRM operates as a generator in flywheel mode. The control is implemented to keep the link voltage at 300 V ($V_{DC}{}^*$), ensuring power to the critical load of 1 kW, which is represented by R_{Ld} resistance of 90 Ω. The voltage controller logic diagram is shown in Figure 12.

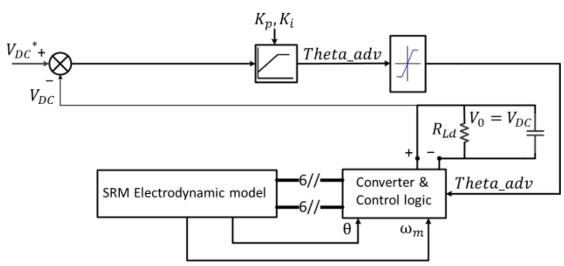

Figure 12: Flywheel voltage controller logic diagram.

To model this mode of operation a 500 µF capacitor represents the DC Link. The capacitor is initially charged with 300 V and is parallel connected with the load. The voltage error serves as the Proportional+Integral voltage controller input, which output is the $Theta\_adv$ advance angle. The $Theta\_adv$

limits are in the range between −15 and 15 mechanical degrees. It is defined as zero in rotor and stator aligned position, is positive in the $L(\theta)$ inductance increase region and is negative in $L(\theta)$ decreasing region, as proposed in (MacMinn, 1989) and shown in Figure 13.
During flywheel operation, the converter switches in single pulse mode. The T_{ij}_1 and T_{ij}_2 switches are ideally closed at the stator and rotor aligned position. The coil current rises to a cut-off value, at this time both switches open and the discharge occurs through D_{ij}_1 and D_{ij}_2, converting rotor's kinetic energy.

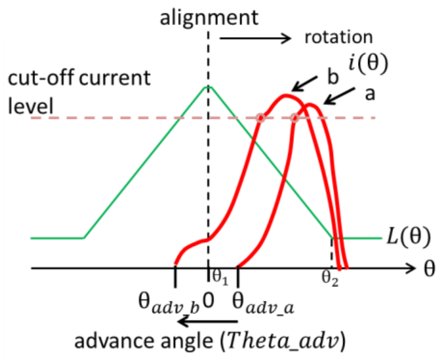

Figure 13: Advance angle variation and its effect on coil current.

7.1 Switched reluctance machine converter control logic in flywheel mode

Figure 14 shows the control logic for one pole's switches during flywheel operation mode.

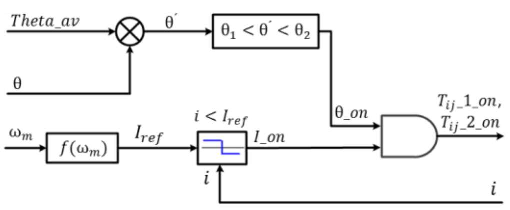

Figure 14: Switched reluctance machine converter control logic in flywheel mode(one pole).

This logic controls T_{ij}_1 and T_{ij}_2 switches to close $Theta\_adv$ mechanical degrees from the beginning of the negative torque region which is defined between θ_1 and θ_2 angles for each pole. Both switches open when i coil current reaches the I_{ref} value. The I_{ref} cut-off value was determined through simulations and varies linearly from 4 to 8 A, for a ω_m speed ranging from 50k to 20k r/min speed variation.

8 Transient simulations

This section presents the transient simulations results obtained in co-simulation between Maxwell and Simplorer, both developed by ANSYS.
Due to the complexity of the analyzed model, in relation to the available computational capability, to perform a full FESS dynamic evaluation, the rotor's moment of inertia given by J in Figure 9 has reduced by a factor of 150. This feature causes an angular acceleration/deceleration 150 times greater than the real one and the time axis is reduced by the same 150 factor.

8.1 Motor operation

These simulations show the SRM ability to accelerate from rest to rated speed within the specified time of 120 s, limiting the applied coil current to a 7 A maximum. Figure 15 shows the electromagnetic torque and Figure 16 shows the angular speed during SRM acceleration.

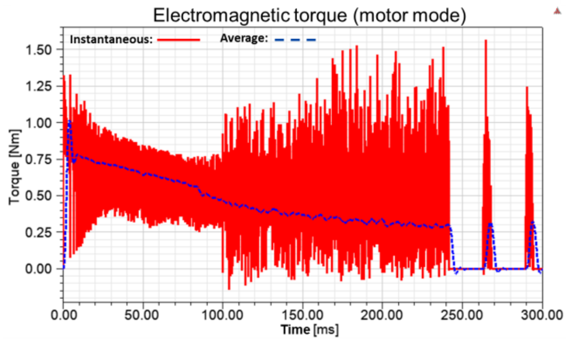

Figure 15: Electromagnetic torque during SRM motor operation.

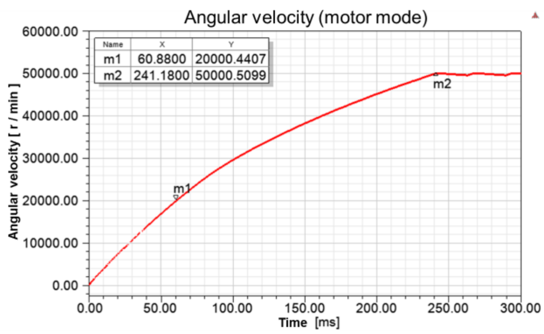

Figure 16: SRM speed acceleration during motor operation.

According to Figure 8, the $\omega_m{}^{*'}$ signal has a 1% hysteresis band. So the final speed is limited between 50k and 49.5k r/min, as shown in Figure 16. The speed acceleration curve gives a time required for the SRM to accelerate from rest to reach 50k r/min of 241 ms, with the scaled-down rotor moment of inertia. For the nominal moment of inertia, the actual acceleration time would be approximately $150 \cdot 0.241$ ms $= 36$ s, according to this simulation.

8.2 Flywheel operation

The following simulations present the FESS discharge characteristics while powering the 1 kW load. The SRM decelerate from 50k r/min. Figure 17 shows the DC Link voltage, load current and control variable ($Theta\_adv$) during flywheel operation mode.

The maximum DC Link observed voltage was 307 V and the time passed until a 10% decrease (to 270 V) in this voltage was about $150 \cdot 200$ ms = 30 s.
Figure 18 shows the SRM angular speed during discharge of kinetic energy in flywheel operation.

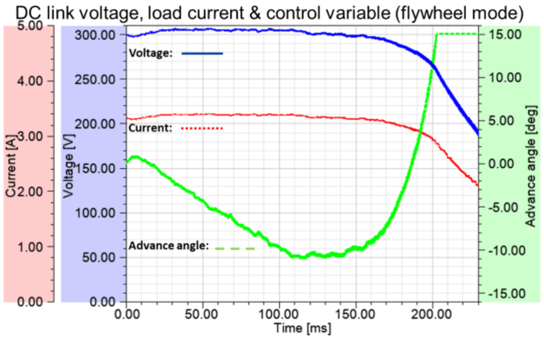

Figure 17: DC Link voltage, load current and control variable during flywheel operation.

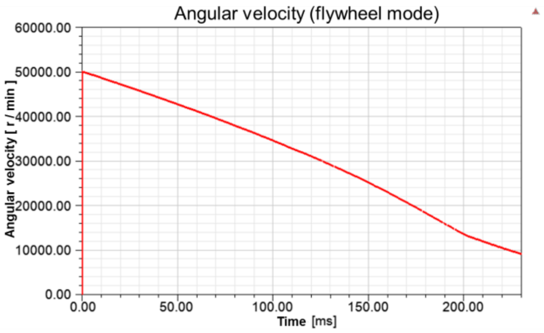

Figure 18: SRM angular speed during flywheel operation.

9 Conclusions

This paper presented the requirements specification, electromagnetic project, machine and control modeling, followed by FEM simulations of an external rotor 6/4 50k r/min SRM applied to a Flywheel Energy Storage System.
While main power supply is online, the projected machine could accelerate from rest to the rated speed in approximately 36 s, faster than initial requirement of 120 s.
When an outage of the main power occurs, the SRM operates as a generator in flywheel mode. It showed a capacity to power the 1 kW resistive load for an estimated time of 30 s, while the requirement was 15 s. The external rotor topology showed a good capacity as a flywheel kinetic energy storer.

Acknowledgments

The authors acknowledge the support provided by the commanders Carvalho and Melo from the Brazilian Navy Research Institute (IPqM-Rio de Janeiro/RJ). We also would like to thank Mr. Dankwart Bernsmüller for translation help.

References

ANSYS. Maxwell [Online]. Available: <http://www.ansys.com/Products/Electronics/ANSYS-Maxwell/Maxwell-Features> Access: Apr./2016.

VYCO ENERGY. VDC-XE [Online]. Available: <http://www.calnetix.com/vycon-direct-connect-xe-products> Access: Dez. 2015.

FERREIRA, C. A., JONES, S. R., HEGLUND, W. S., JONES, W. D. 1995. Detailed design of a 30-kW switched reluctance starter/generator system for a gas turbine engine application. Industry Applications, IEEE Transactions on, Vol. 31, 553-561.

KRISHNAN, R. 2001. Switched Reluctance Motor Drives: Modeling, Simulation, Analysis, Design and Applications, Boca Raton, CRC Press LLC, 2001.

MACMINN, S. R., SEMBER, J. W. Control of a switched-reluctance aircraft engine starter-generator over a very wide speed range. Energy Conversion Engineering Conference, 1989. IECEC-89., Proceedings of the 24th Intersociety, 6-11 Aug 1989 1989. 631-638 vol.1.

MILLER, T. J. E. 1993. Switched Reluctance Motors and Their Control, Oxford, Magna Physics Publishing/Clarendon Press, 1993.

A. S. Ortiz, "Magnetic bearings applied to induction motors using the same stator coils (Mancais magnéticos para motores de indução utilizando os próprios enrolamentos de estator)" M.Sc Dissertation, COPPE/UFRJ, Rio de Janeiro, RJ, Brazil, 1989.

ACTIVE POWER. CleanSource 300 [Online]. Available: <http://www.activepower.com/cleansource-300/#300specs> Access: Dez. 2015.

POWERTHRU. Clean Flywheel Energy Storage [Online]. Available: <http://www.power-thru.com/documents/POWERTHRU.pdf> Access: Dez. 2015.

SCHWEITZER, G. 2002. Active magnetic bearings - chances and limitations. International Centre for Magnetic Bearings, ETH Zurich.

SHOUJUN, S., WEIGUO, L., PEITSCH, D., SCHAEFER, U. 2010. Detailed Design of a High Speed Switched Reluctance Starter/Generator for More/All Electric Aircraft. Chinese Journal of Aeronautics, Vol. 23, 216-226.

ZANEI, G., CEVENINI, E., RUFF, H. & ULIBAS, O. Integrated systems for UPS: New solutions in the power quality chain. Telecommunications Energy Conference, 2007. INTELEC 2007. 29th International, Sept. 30 2007-Oct. 4 2007. 582-586.